Available online at www.sciencedirect.com
ScienceDirect
Atmospheric Environment 41 (2007) 5605–5617
ATMOSPHERIC ENVIRONMENT
www.elsevier.com/locate/atmosenv

Area of influence (AOI) sensitivity analysis: Application to Atlanta, Georgia

Sergey L. Napelenok[a,*,1], Florian D. Habermacher[b], Farhan Akhtar[c], Yongtao Hu[a], Armistead G. Russell[a]

[a]*Department of Civil and Environmental Engineering, Georgia Institute of Technology, Atlanta, Georgia 30332, USA*
[b]*Environmental Sciences and Engineering Section, Swiss Federal Institute of Technology in Lausanne, 1015 Lausanne, Switzerland*
[c]*School of Earth and Atmospheric Science, Georgia Institute of Technology, Atlanta, Georgia 30332, USA*

Received 13 September 2006; received in revised form 1 January 2007; accepted 1 March 2007

Abstract

Area of influence (AOI) analysis was applied to determine the geographical extent of the air pollutant precursors contributing to various pollutant levels in the Atlanta metropolitan area. Receptor-oriented sensitivities of ozone and particulate matter (PM) species to emissions of NO_x, SO_2, NH_3, anthropogenic VOC, and elemental carbon were calculated for various combinations of precursor emissions during 1–10 August, 1999. The episode had high observed concentrations of ozone and PM across several days. AOIs differed significantly by day for each sensitivity as well as spatially between pollutants. Ozone sensitivities peaked at 1.0 ppb per 1.0 mole s^{-1} (or per 4.0 ton day^{-1}) per $12 \times 12\,km^2$ model grid of emissions of NO_x, but averaged around 0.1 ppb over much of Atlanta. Sulfate was the major component of PM, with an average sensitivity of 0.03 μg m^{-3} per 1.0 mol s^{-1} (or per 5.5 ton d^{-1}) per $12 \times 12\,km^2$ model grid of SO_2 emissions and an average of 0.02 μg m^{-3} per 1.0 mol s^{-1} per $12 \times 12\,km^2$ of NO_x emissions. Ammonia had a significant impact on PM through the formation of ammonium sulfate and ammonium nitrate. Elemental carbon had a geographically small area of influence with high values around the receptor.

Keywords: Area of influence; AOI; Sensitivity analysis; Atmospheric modeling; Air quality; Direct decoupled method

1. Introduction

Air quality has improved over the last decade in the United States and Europe; however, there are still regions where large segments of the population are exposed to elevated levels of ozone and particulate matter (US-EPA, 2004). Both have been linked to negative impacts on human health (Dockery et al., 1993; Pope et al., 2002). In order to control these pollutants, it is important to identify sources and source regions leading to elevated levels. Ozone and PM concentrations have been simulated using three-dimensional, emissions based air quality models such as CMAQ and CAMx, which spatially and temporally resolve these and many other species with good accuracy compared to actual

*Corresponding author. Tel.: +1 919 541 1135.
E-mail address: Napelenok.Sergey@epa.gov (S.L. Napelenok).
[1]Currently at Atmospheric Sciences Modeling Division, Research Triangle Park, NC, USA.

1352-2310/$ - see front matter © 2007 Elsevier Ltd. All rights reserved.
doi:10.1016/j.atmosenv.2007.03.006

measurements (Russell and Dennis, 2000). Recently, these models were extended to provide sensitivities of air pollutants in addition to concentrations using the decoupled direct method (DDM) (Yang et al., 1997; Dunker et al., 2002a,b; Cohan et al., 2005; Napelenok et al., 2006), as well as adjoint approaches (Hakami et al., 2006). Sensitivity analysis has a wide array of applications ranging from source apportionment (Dunker et al., 2002a,b; Boylan et al., 2004; Cohan et al., 2005), control strategy assessment, and estimation of uncertainty (Fine et al., 2003).

DDM calculates source impacts in a "forward" sense by providing the response of one or more receptors to perturbations in input parameters at the sources (emissions, initial/boundary conditions, etc.). Adjoint analysis provides receptor-oriented sensitivities, where perturbations are originated at a receptor of interest and propagated backwards in time (Sandu et al., 2005; Hakami et al., 2006). While currently only available for gas phase species, this method is useful in identifying which sources of air pollution precursors influence a particular receptor, such as densely populated urban area or a protected national park. However, the adjoint method is computationally costly to operate and is most efficient for a large number of receptors. As an alternative, the area of influence (AOI) method was developed that provides similar information along with forward sensitivities (Habermacher et al., 2007). AOI calculation takes advantage of the ability of DDM to efficiently calculate several source-based sensitivities at once. The forward sensitivities are spatially interpolated and inverted to provide receptor-oriented AOIs. Additionally, the computational investment in obtaining AOI fields at any number of receptor is minimal after the forward DDM fields are developed.

Combined with concentrations and sensitivities already calculated by current air quality models, AOIs provide additional information on air quality within a region. AOI analysis was applied to calculate receptor-oriented ozone and particulate matter sensitivities in Atlanta, Georgia. Atlanta and its surrounding suburbs are home to over four million people, and have elevated levels of zone and particulate matter with aerodynamic diameter of less than 2.5 μm ($PM_{2.5}$). Area of influence analysis is ideal for a place like Atlanta, where it is necessary to develop a clear understanding of where emissions of precursors to ozone and particulate matter formation have the greatest impacts, along with the impacts of specific sources (e.g., Cohan et al., 2005; Napelenok et al., 2006).

2. Method

2.1. Area of influence (AOI)

Described in more detail elsewhere (Habermacher et al., 2007), the AOI method is used to generate receptor-based sensitivity fields from forward sensitivities developed using DDM. The AOI of a pollutant i at a receptor $\overline{x}_r$ to emissions of j, or $Z_{ij,r}(\overline{x}, t)$, is expressed by the following:

$$Z_{ij,r}(\overline{x}, t) = \frac{\partial C_i(x_r, t)}{\partial E_j(\overline{x_s})} \quad (1)$$

where $E_j(\overline{x}_s)$ is non-dimensional perturbation of the constant emissions of species j at location $\overline{x}_s$. AOIs provide relative receptor-based sensitivities to potential emissions at any point, not actual emissions, e.g., the additional amount of pollutant formed if emissions were increased by the specified amount. $Z_{ij,r}(\overline{x}, t)$ is developed by calculating source-based sensitivity field to constant emissions at pre-selected locations in the modeled domain, interpolating these fields to all locations, and then Eq. (1) is used to obtain receptor-based sensitivity fields or the AOI, which will be referred to as inverting (see more extensive discussion in Habermacher et al., 2007).

2.2. Application

AOI analysis was applied to a domain centered on Atlanta, Georgia (Fig. 1). A 57×60 cell grid with 12 km resolution was nested within a larger 36 km resolution grid used for providing boundary conditions. A similar domain was used previously for the Fall Line Air Quality Study (FAQS) (Hu et al., 2004). A 10 day summer episode was selected: 1–10 August, 1999. During this period, Atlanta and much of the rest of the state experienced periods of highly elevated ozone and particulate matter levels. Meteorology for the episode was developed using Mesoscale Meteorological Model version 5 (MM5) (PSU/NCAR, 2003). Emissions were developed from FAQS inventories (Hu et al., 2004) and processed using SMOKE version 2.2 (CEP, 2004). An instrumented version of the Community Multiscale Air Quality (CMAQ) model version 4.3 (Byun and Schere, 2006) capable of computing sensitivities using the DDM method (Cohan et al., 2005;

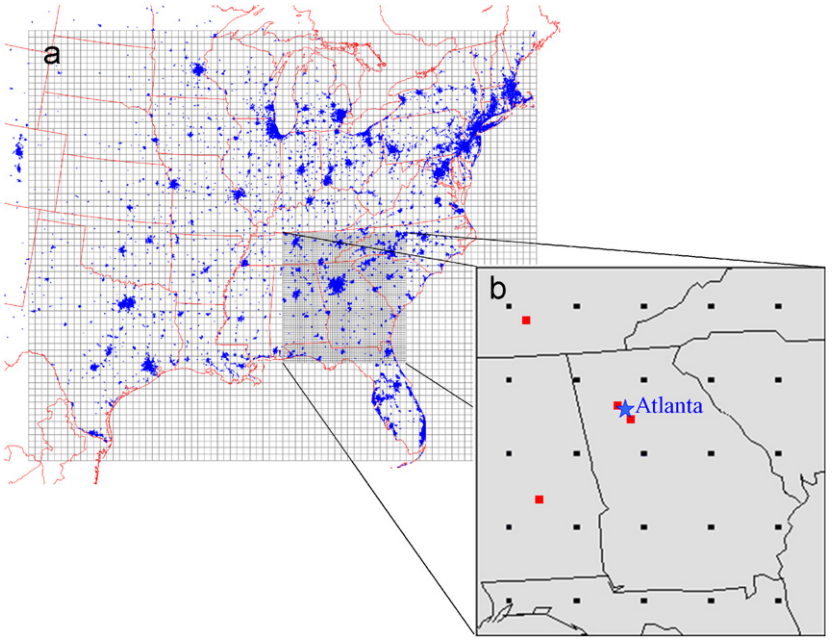

Fig. 1. Domain used for AOI analysis. (a) The larger coarse grid is 78 × 66 with 36 km resolution and the smaller nested grid is 57 × 60 with 12 km resolution and 13 vertical layers. Urban areas are distinguished by the blue areas. (b) Distribution of the pre-selected sources of forward sensitivities is shown as black dots. Sensitivities to emissions of various pollutants were calculated as point sources at these 25 locations and later interpolated for the rest of the grid cells in the domain. Red dots denote the four additional locations used for the refined analysis.

Napelenok et al., 2006) was used to develop concentration and source-based sensitivity fields.

Initial forward sensitivity fields were developed for 25 regularly spaced grid cells within the domain (Fig. 1) and extrapolated to the rest of the cells (Habermacher et al., 2007). Sensitivities to emissions of SO_2, NO_x, NH_3, anthropogenic VOC, and elemental carbon were calculated. Species examined included ozone, sulfate, nitrate, particulate elemental carbon, anthropogenic secondary organic aerosol, and total $PM_{2.5}$ (particulate matter with aerodynamic diameter less than 2.5 μm). For ozone, AOIs were calculated for the 8-h average at the time of peak concentration, and 24-h averages were computed for $PM_{2.5}$.

The simulated episode had high observed ozone and $PM_{2.5}$ concentrations. Stagnant air was trapped in the region for an extended period of time due to a high pressure system situated directly over the southeastern United States. The resulting low speed winds, high temperature, and little precipitation coupled with high emissions in the region presented ideal conditions for poor air quality. Ozone was high around the Atlanta metropolitan area on all days with an observed peak 8-h average concentration of 139 ppb on 4 August, 1999. Observed 24-h average $PM_{2.5}$ concentrations in Atlanta were also high throughout the episode.

3. Results and discussion

Model performance was evaluated before beginning AOI analysis to insure reasonable results. Simulated concentrations of ozone and each particulate species were compared to observed values from the aerometric information retrieval system (AIRS) and interagency monitoring of protected visual environments (IMPROVE) sites in the domain (US-EPA, 1993; NPS, 2006). Ozone had a mean normalized error of 20.3% and a mean normalized bias of −2.69%. Both of these statistics are well within the EPA's guidelines for air quality modeling (US-EPA, 1999). Aerosol model performance was calculated based on the methods outlined by Boylan et al. (2004). $PM_{2.5}$ had a fractional error of 28.5 and a fractional bias of −13.0. Individual $PM_{2.5}$ components also performed similarly (Table 1), with the exception of nitrate, which had much higher fraction error (103.4), but was present in very low quantities (average of 0.6 $\mu g\,m^{-3}$

Table 1
Particulate matter modeling performance for the 1–10 August, 1999 episode

	Average observed concentration[a] ($\mu g\,m^{-3}$)	Fractional error	Fractional bias
Total $PM_{2.5}$	29.1	28.5	−13.0
Sulfate	10.3	30.7	2.72
Nitrate	0.6	103.4	−78.8
Ammonium	4.4	37.3	−26.7
Elemental carbon	1.4	52.0	−9.3
Organic carbon	7.6	50.3	−41.6

[a]Concentration averages are computed for monitoring stations with available observations.

at all available stations in the domain). Organic carbon was underestimated. Overall, $PM_{2.5}$ performance was similar to that reported by other studies (Boylan et al., 2004; Seigneur et al., 2004). The performance of DDM-3D in CMAQ (Cohan et al., 2005; Napelenok et al., 2006) and the AOI method (Habermacher et al., 2007) have been evaluated elsewhere.

Simulated fields show extensive areas of elevated ozone (Fig. 2) that were found to be consistent with observations. $PM_{2.5}$ was more uniform throughout the domain with a dramatic peak on 7 August of $79.8\,\mu g\,m^{-3}$ in Atlanta (Fig. 3). Sulfate and "unspecified" mass composed the largest fraction (20% and 35%, respectively). Elemental and organic carbon contributed around 15% each while secondary organic aerosol (SOA) and ammonium contributed around 10% each.

3.1. Ozone area of influence

Due to large amounts of emissions of biogenic VOCs in the region, ozone formation around the Atlanta metropolitan area is usually NO_x limited. Prior sensitivity results (Cohan et al., 2005) show a very limited area of VOC emissions impacting ozone. Thus, the ozone AOI for NO_x emissions is discussed here. Forward fields for ozone were developed as sensitivities to an addition of continuous emissions of $1.0\,mole\,s^{-1}$ (or approximately $4.0\,ton\,day^{-1}$) per $12 \times 12\,km^2$ model grid of NO_x at each of the 25 regularly spaced sources in the domain. These kinds of emissions are equivalent to a concentrated point source or an area source of the same net strength within the model grid. The perturbation in emissions resulted in a plume of ozone sensitivities that developed over time originating from each source location (Fig. 4). A running 8-h average was computed for all ozone results to correspond to the averaging period of the National Ambient Air Quality Standards (NAAQS). Forward sensitivities for ozone captured titration of ozone by NO_x during the night, resulting in negative sensitivities near the sources during periods without sunlight. As photochemical activity increased, forward sensitivity plumes shifted to positive values. Large variability exists between individual forward fields as well as within each field temporally suggesting complex meteorological and chemical interactions of NO_x to produce ozone in the region. The forward ozone sensitivities range from around $-10\,ppb$ ozone at night to $+10\,ppb$ ozone during the day per $1.0\,mole\,s^{-1}$ per $12 \times 12\,km^2$ model grid continuous emissions of NO_x.

After the interpolation and the inversion procedures, the area of influence results for Atlanta show significant daily variability (Fig. 5). The highest contribution to ozone formation by NO_x appears in regions near the receptor. However, on days where concentrations were particularly high (5, 7 August), longer range transport from the rest of Georgia and the neighboring states is evident. In some grid cells, AOI reaches as high as $1.0\,ppb$ ozone per $1.0\,mole\,s^{-1}$ per $12 \times 12\,km^2$ model grid continuous NO_x emissions. However, most of the contribution comes from cells with magnitudes of around 0.1 ppb. Daily variability is also drastic in the AOI plots suggesting that control strategies employing sensitivity analysis will require several days of results in order to get a representative sample.

In order to evaluate the AOI results, the HYbrid single-particle Lagrangian integrated trajectory (HYSPLIT) model (Draxler and Rolph, 2003), driven by the global reanalysis meteorological data set, was used to compute reverse wind trajectories from Atlanta (Fig. 6). While HYSPLIT results neglect chemical interactions accounted for in CMAQ, they are useful in identifying the spatial progression of air parcels that arrive at the receptor during the time of peak ozone. In this case, the trajectories support the general patterns of the AOI plots. On 3 August, the ozone area of influence stretches in the northeasterly direction through South Carolina as do the reverse wind trajectories. However, 5 August and 7 August show evidence of low speed winds with frequently changing

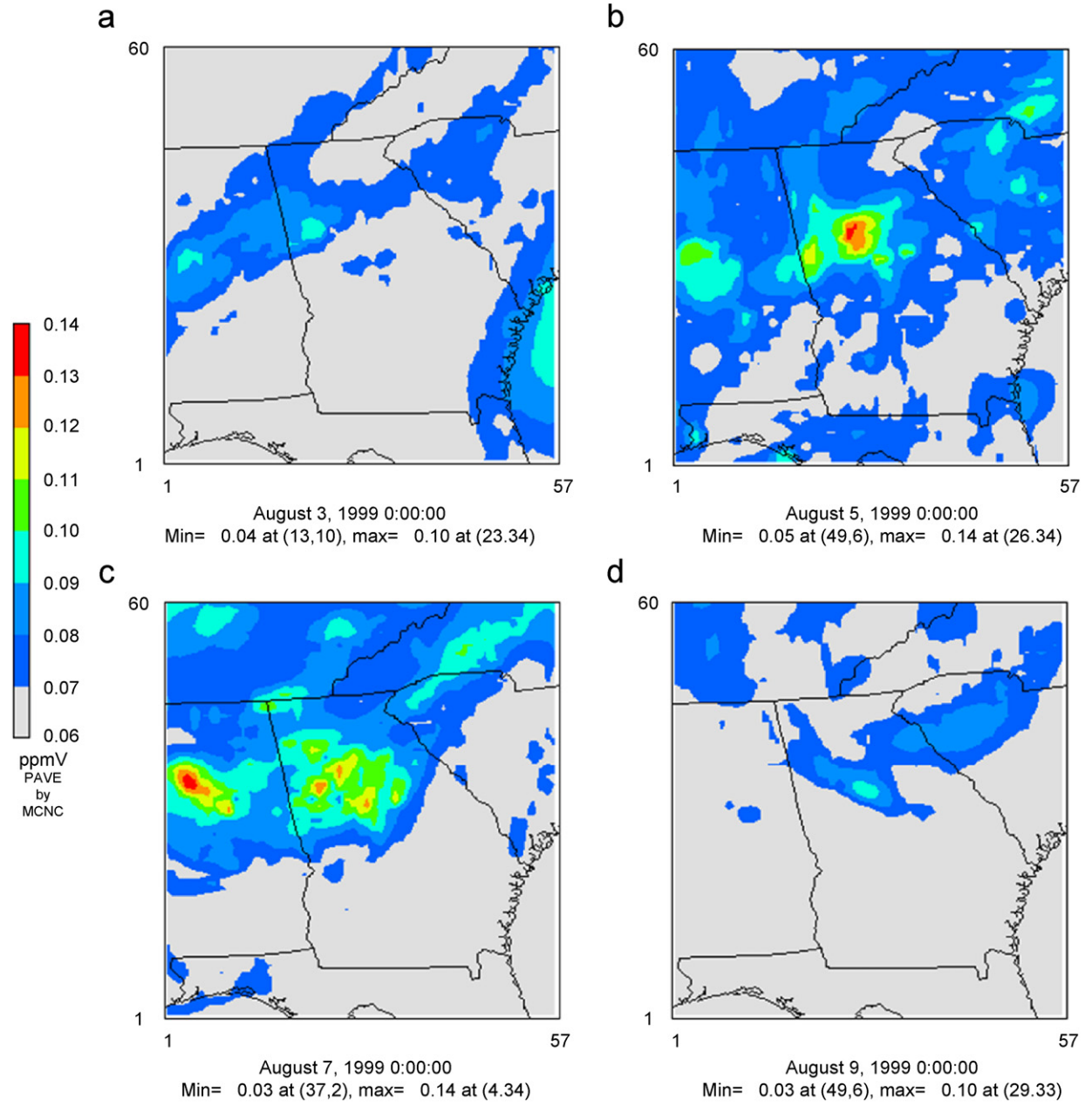

Fig. 2. Simulated maximum daily 8-h ozone concentrations for (a) 3 August, (b) 5 August, (c) 7 August, and (d) 9 August, 1999. Observed and simulated concentrations exceeded the 8-h NAAQS of 0.08 ppm for ozone each day.

directions. These two days had higher ozone concentrations due to stagnation. Ninth August shows fairly constant winds coming from Alabama and the AOI has a similar direction of the sources for NO_x that led to ozone formation in Atlanta on that day. Trajectories for all days had very little vertical movement.

3.2. Particulate matter area of influence

Sensitivities of total particulate matter, as well as its individual components, were calculated for potential emissions of SO_2, NO_x, NH_3, anthropogenic VOC, and elemental carbon. Since 7 August was such an extreme peak in simulated $PM_{2.5}$

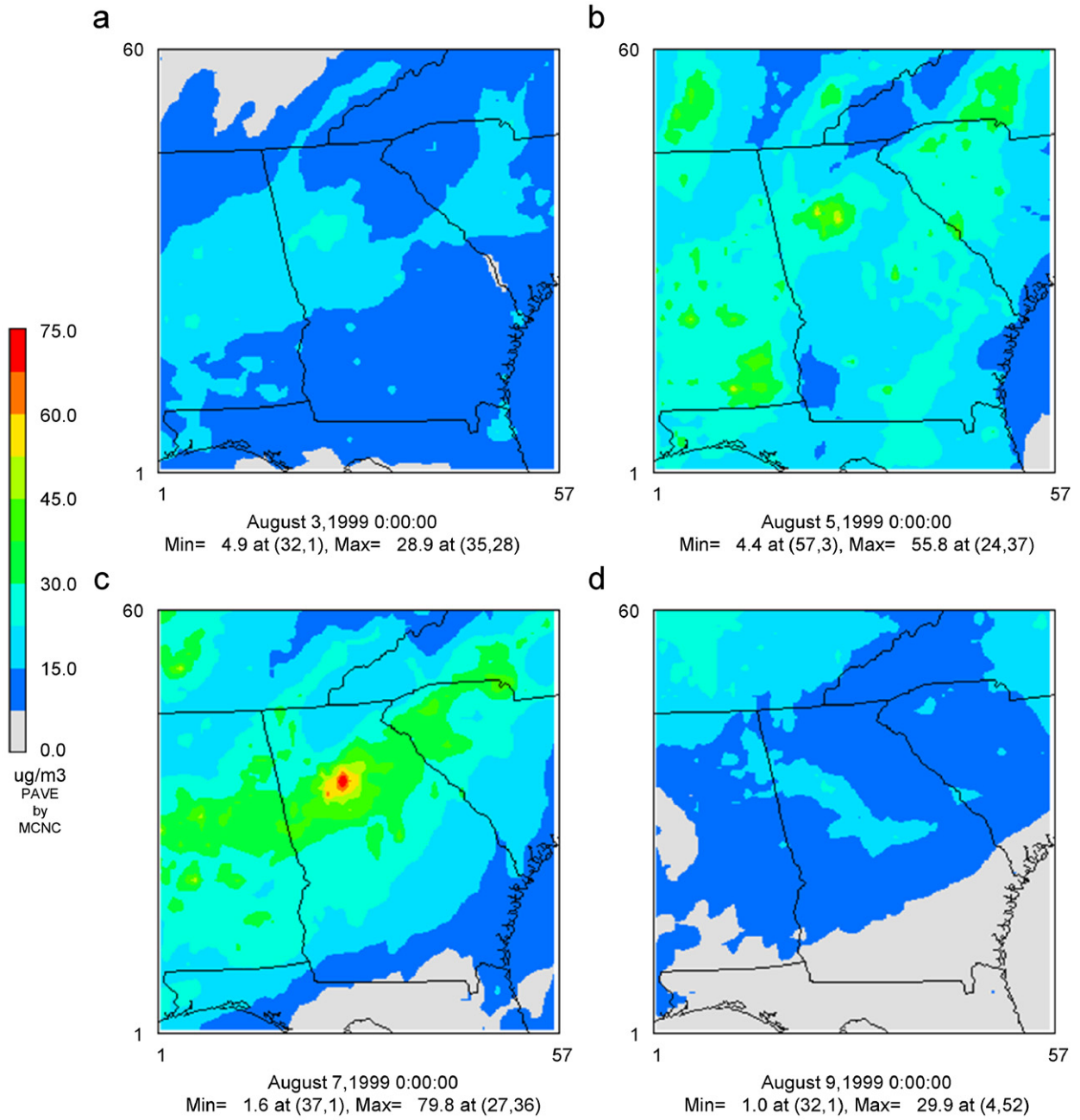

Fig. 3. Simulated 24-h averaged $PM_{2.5}$ concentrations for (a) 3 August, (b) 5 August, (c) 7 August, and (d) 9 August, 1999. $PM_{2.5}$ is the sum of Aitken and accumulation modes of sulfate, nitrate, ammonium, elemental carbon, primary and secondary organic carbon, and "unspecified" aerosol. Simulated concentrations exceeded the daily averaged NAAQS of 65 $\mu g\,m^{-3}$ on the 7th and were well above the annual averaged standard each day.

concentrations, AOIs for this day were analyzed (Fig. 7). Similar to the ozone AOI on this day, a large amount came from south of Atlanta, though, shifting low speed winds during a part of the day led to potential contributions from the north. Sulfate is an important $PM_{2.5}$ component in this region due to SO_2 emissions. The area of influence of sulfate sensitivity to SO_2 emissions is large suggesting the regional nature of this pollutant (Fig. 7a). This AOI reached a maximum of 0.1 $\mu g\,m^{-3}$ sulfate sensitivity

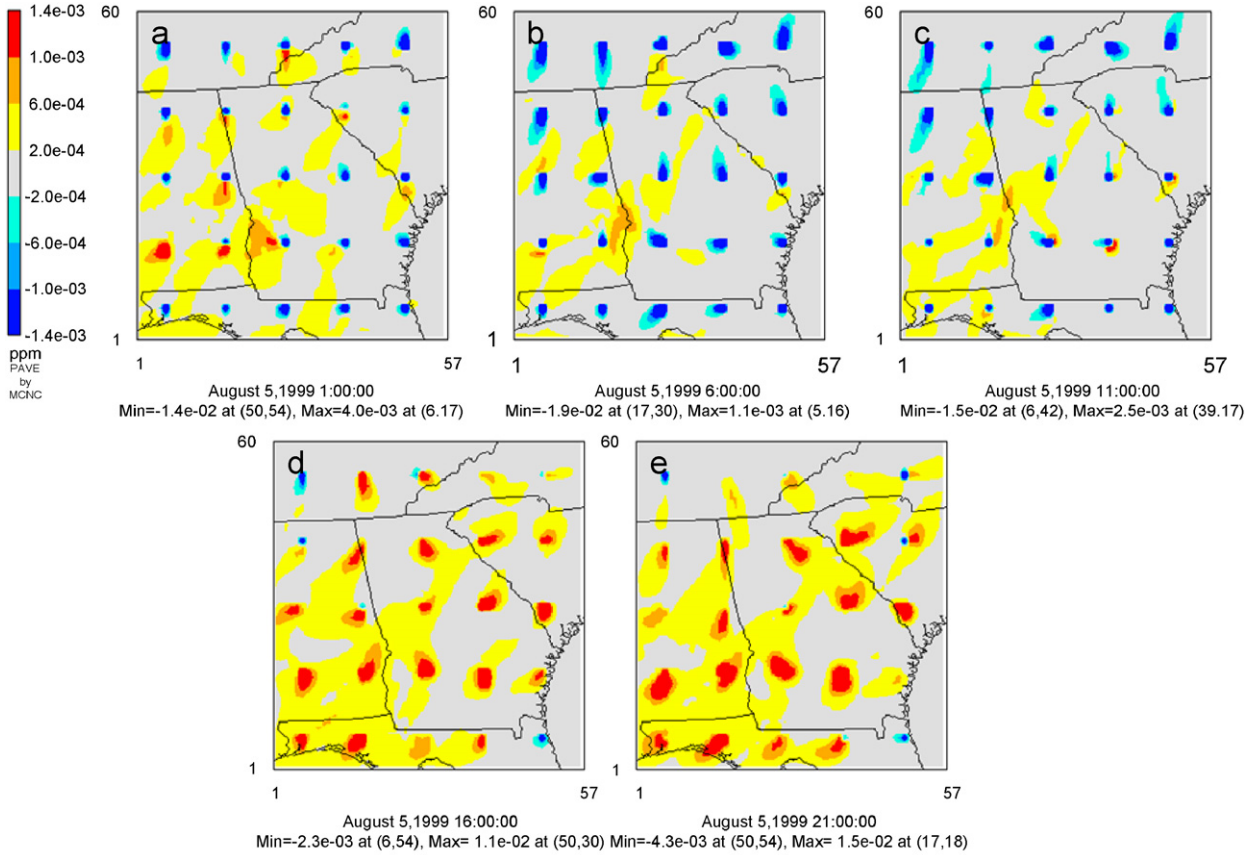

Fig. 4. Ground level forward fields of ozone sensitivity to domain-wide NO_x emissions on 5 August, 1999 at (a) 01:00, (b) 06:000, (c) 11:00, (d) 16:000, and (e) 21:00 (8-h average). Sensitivities are computed to a 1.0 mole s^{-1} increase in NO_x emissions at each location. The 25 fields were computed independently, but are presented as a summation. Blue areas indicate ozone titration by NO_x during night-time, while the red areas represent the formation of ozone in the presence of sunlight.

per mole s^{-1} (or per 5.5 ton day^{-1}) per $12 \times 12\,km^2$ model grid of SO_2 emissions, but generally ranged from 0.02 to 0.05 $\mu g\,m^{-3}$. NO_x emissions act to facilitate the oxidation of SO_2 and the subsequent formation of sulfate. However, this effect is less important and thus the AOI for sulfate sensitivity to NO_x emissions shows lower level of impact (0.02 $\mu g\,m^{-3}$ sulfate per 1 mole s^{-1} NO_x emissions (Fig. 7b)). While SOA produced from biogenic sources is dominant in the region, anthropogenic precursors were considered in the AOI analysis as these are more open to control. Sensitivities to VOC emissions are fairly low, averaging around 0.001 $\mu g\,m^{-3}$ per mole s^{-1} per $12 \times 12\,km^2$ model grid of SOA sensitivity (Fig. 7c). Ammonium emissions, on the other hand, are responsible for a significant fraction of secondary particulate matter produced in the region with peak AOI sensitivity of 2.4 $\mu g\,m^{-3}$ and averaging around 0.1 $\mu g\,m^{-3}$ (Fig. 7d). The overall sensitivity of $PM_{2.5}$ to ammonia emissions is large, so NH_3 emissions control should be considered in regional control strategies (Fig. 7e). Effects of primary emissions were considered by calculating the AOI of elemental carbon emissions to elemental carbon concentrations in Atlanta (Fig. 7f). The AOI for elemental carbon shows high values peaking at 5.4 $\mu g\,m^{-3}$ per $g\,s^{-1}$ per $12 \times 12\,km^2$ model grid, however, the spatial extent of high sensitivity around Atlanta is fairly small. EC levels are typically high in areas very near its emission due to dispersion (Kim et al., 2002), which is confirmed by the AOI analysis. Other non-reacting aerosol species would have similar AOIs.

3.3. Upper level emissions

AOI results presented above show the expected changes in concentrations in Atlanta due to

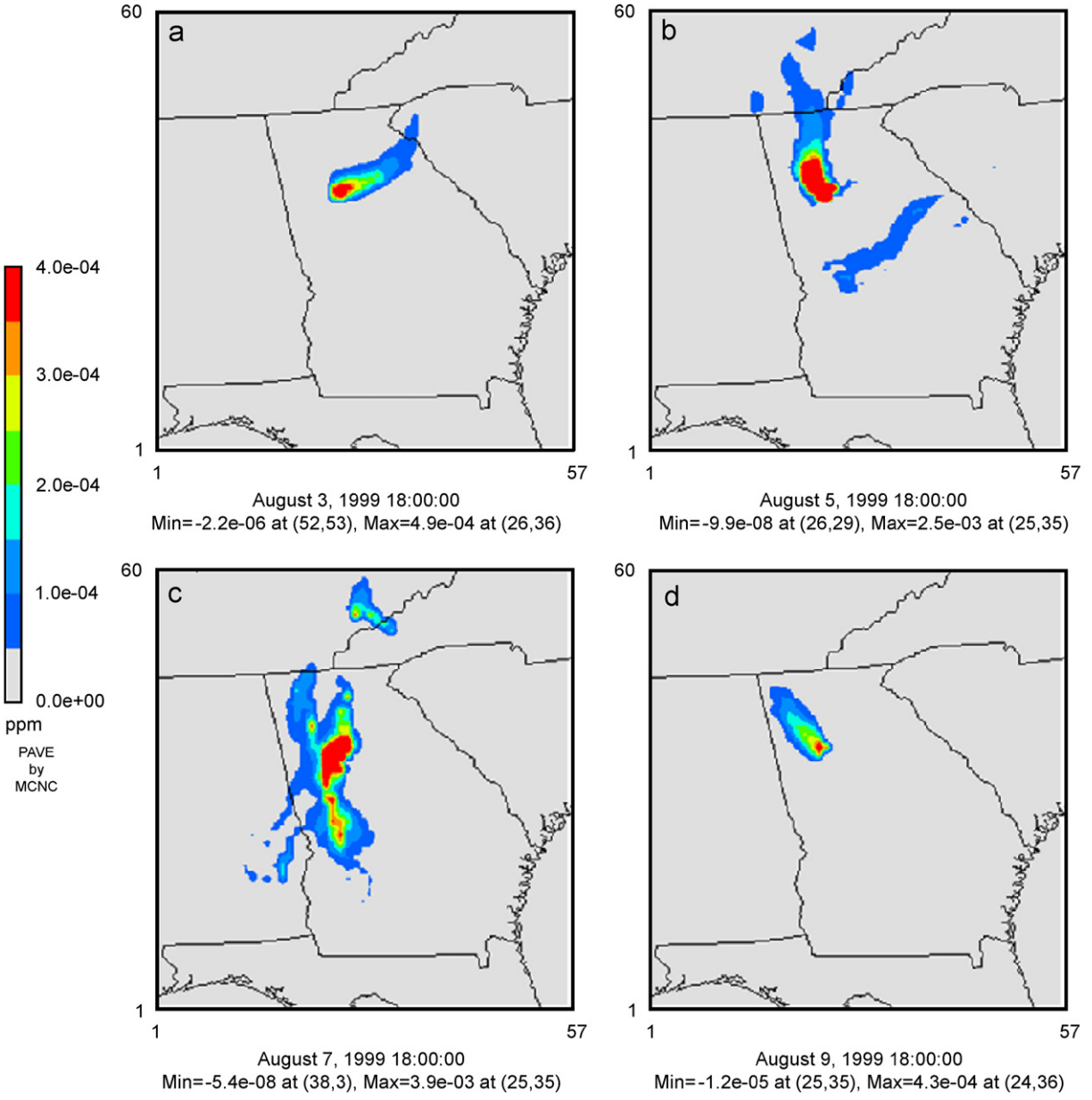

Fig. 5. Ground level ozone area of influence (AOI) from ground level emissions of NO_x on (a) 3 August, (b) 5 August, (c) 7 August, and (d) 9 August, 1999 in Atlanta. Results are shown for the 8-h average at 18:00 on each day. The AOI shows the impact that a mole s^{-1} NO_x source at that location would have on ozone at the Atlanta receptor site. Thus, adding a 1 mole s^{-1} NO_x source in an area that corresponds to 0.25–0.30 ppb (yellow) would lead to a 0.25–0.30 ppb increase in Atlanta ozone.

changes in emissions in the lowest 20 m of the domain (model layer 1). Some emissions also occur in the upper levels. For example, SO_2 from electricity generating units (EGUs) is effectively released at around 500 m due to high temperatures and exit velocities from power plant stacks. AOIs at the ground level to upper level emissions of SO_2 were also calculated (Figs. 8a and c). On most days, there is little difference between the upper layer and the ground level AOIs. For example, on 7 August, the ground level AOI shows a higher maximum and stronger influence from eastern Tennessee (Fig. 7a), while the upper level AOI has more areas with a high influence from Georgia (Fig. 8c), but a lower peak sensitivity.

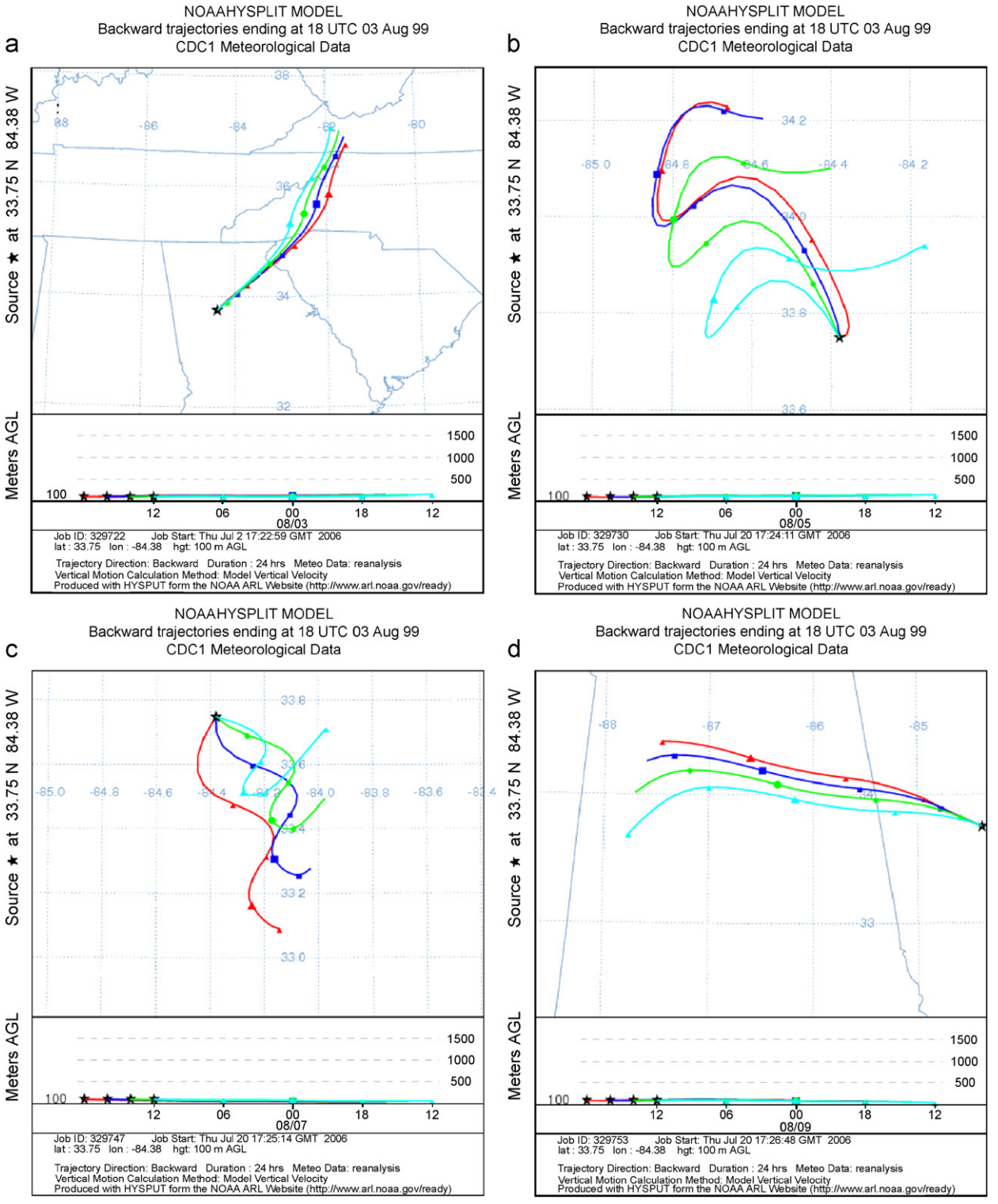

Fig. 6. Reverse wind trajectories as computed by the HYSPLIT model (Draxler and Rolph, 2003) on (a) 3 August, (b) 5 August, (c) 7 August, and (d) 9 August, 1999. The 100 m, 24 h trajectories are shown arriving in Atlanta at 18:00 (red), 16:00 (dark blue), 14:00 (green), 12:00 (light blue). While (a) and (d) show fairly constant winds, the other two days evidently experienced frequent changes in wind direction which is reflected in the AOI results.

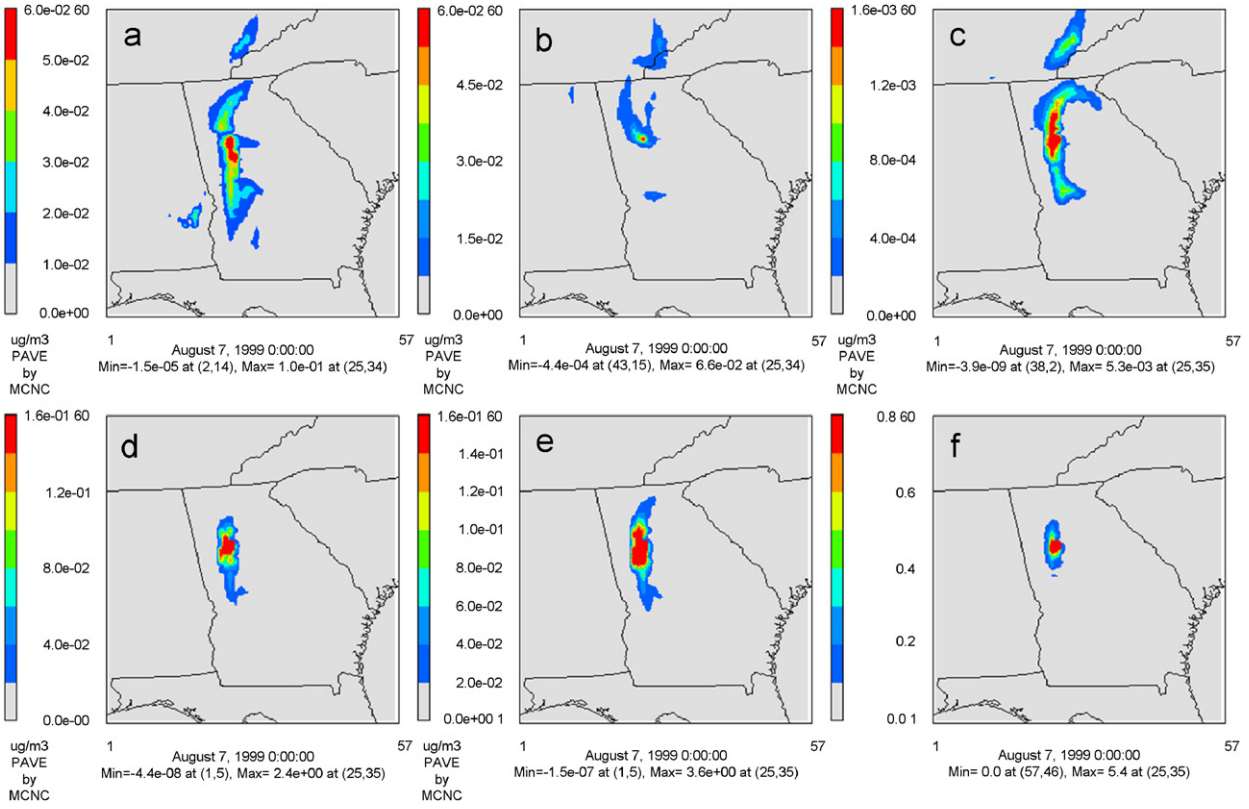

Fig. 7. Ground level area of influence (AOI) on 7 August, 1999 of (a) sulfate to ground level SO_2 emissions, (b) sulfate to ground level NO_x emissions, (c) SOA to ground level anthropogenic VOC emissions, (d) ammonium to ground level NH_3 emissions, (e) total $PM_{2.5}$ to ground level NH_3 emissions, and (f) elemental carbon to ground level elemental carbon emissions. All results are 24-h averaged. The AOI shows the impact that a mole s^{-1} of the specified pollutant source at that location would have on ozone at the Atlanta receptor site. Thus, adding a 1 mole s^{-1} SO_2 source in an area of (a) that corresponds to 3.0−4.0 $\mu g\,m^{-3}$ (green) would lead to a 3.0−4.0 $\mu g\,m^{-3}$ increase in Atlanta sulfate.

In order to quantify the current spatial contributions of sensitivity to Atlanta, the product of the AOI field for sulfate sensitivity to SO_2 and the actual emissions field of SO_2 in the appropriate level ($Z_{ASO_4^{2-},SO_2,ATL}(\bar{x},t) \cdot E_{SO_2}(\bar{x},t)$) was calculated. It was found that sulfate sensitivity to upper level SO_2 emissions are spatially distributed such that the peaks do not always correspond with the AOI peaks on most days (Figs. 8b and d). This is possible because the emission peaks during this episode occurred in the area where AOI shows only smaller sensitivities. However, if at any time the emission peaks coincide with AOI peaks, the impacts would be substantial.

3.4. AOI iteration

AOI analysis can be further improved by increasing the number of initial forward sensitivity "seed" points and also by developing a better system of determining their locations. In the results shown above, 25 points were located in a regularly spaced grid over the domain. However, several of these points are located in areas of low emissions far away from the target receptor making their contributions insignificant. Four additional points were added in cells (25 35), (11 22), (10 50), and (24 37) (Fig. 1b). The addition had a minor impact on the spatial extent of the AOI, but a significant improvement on the ability to capture local sensitivities.

In order to quantify the improvement in performance of AOI, the following relationship was used:

$$\sum_{c=1}^{N} Z_{ij,r}(\bar{x}_c,t) \cdot E_j(\bar{x}_c,t) = S_{ij}(\bar{x}_r,t), \tag{2}$$

where $Z_{ij,r}(\bar{x}_c,t)$ is the AOI field of pollutant i from emissions of j at each cell c in the domain (out of the total N), $E_j(\bar{x}_c,t)$ is the emissions of j in that cell,

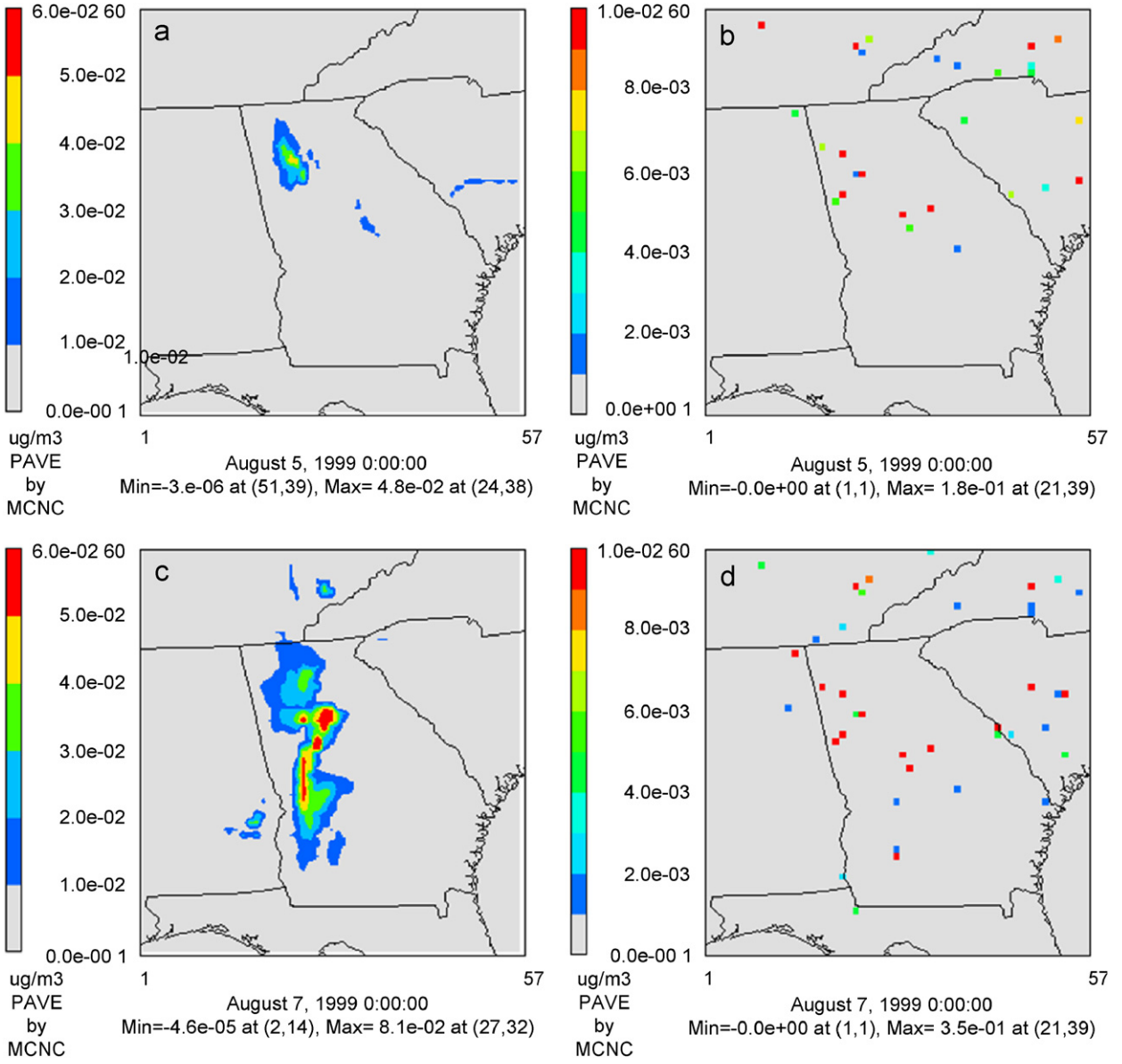

Fig. 8. Ground level area of influence on (a) 5 August and (c) 7 August, 1999 of sulfate to SO_2 emissions at 500 m and the corresponding day's—(b), (d)—contribution of the same sensitivity (calculated as the product of emissions at 500 m and the corresponding AOI). All results are 24-h averaged.

and $S_{ij}(\overline{x}_r, t)$ is the sensitivity of i to domain-wide emissions of j at the receptor location r for which the reverse field was developed. Adding up the product of the emissions in each cell and that cell AOI contribution should approximately equal the sensitivity in that cell to domain-wide emissions if forward fields were developed from each cell and not interpolated. (The interpolation procedure used limits the maximum sensitivities, so it is expected that this test would be biased low.) In essence, the source-based sensitivity field is a collection of receptor-based fields at each location in the domain and vice versa, and Eq. (2) is used to evaluate consistency. The results suggest that the addition of just four well-placed forward fields improve the performance significantly. Averaged over the entire length of the episode, 72% of the sulfate sensitivity in Atlanta to ground level emissions of SO_2 domain-wide was accounted for using the AOI results and Eq. (2) with the extra 4 points compared to 64%

Table 2
AOI performance evaluation for sulfate sensitivity in Atlanta to domain-wide emissions of SO_2 at the ground level

Date	Sensitivity ($\mu g\,m^{-3}$)	Predicted fraction (%) (25 points)	Predicted fraction (%) (29 points)
2 August	0.27	67.1	72.6
3 August	0.12	67.1	71.1
4 August	0.22	60.8	64.9
5 August	0.24	56.9	83.3
6 August	0.46	57.1	68.4
7 August	0.44	65.2	78.4
8 August	0.26	78.2	71.9
9 August	0.27	60.4	68.7

AOI predicts a higher fraction of the expected sensitivity with four additional points some of which are located up-wind and in areas of high SO_2 emissions.

calculated in the same way using the original 25 points (Table 2). Thus, the method can be used in an iterative fashion with low additional computational resource investment if higher resolution results are desired.

4. Summary

The expanding Atlanta metropolitan area has high mobile and industrial emissions in addition to being surrounded by several coal-fired power plants and biogenic VOC emissions from the vegetation covering a large fraction of the region. This complex mixture of different pollutants in the same location leads to both high ozone and high PM concentrations. Determining the sources of these pollutants is further complicated by complex and variable meteorology. Area of influence analysis as applied to Atlanta provides the geographical extent of the sources that led to formation of both ozone and $PM_{2.5}$ during the 1–10 August, 1999 episode. AOI analysis was done on a per mole s^{-1} basis in order to show how much concentrations in Atlanta would change due to a specific increase in emission at any location in the domain. For example, if a 2 mole s^{-1} source of NO_x is added in an area where the AOI value is 0.02 ppb per mole s^{-1}, the resulting increase in 8-h ozone in Atlanta would be 0.04 ppb. It was found that while all sensitivity had significant daily variation some had a large footprint (sulfate formation from SO_2), while other had only local effects (elemental carbon). Further variation is evident from the effect on the ground level receptors from elevated sources. Sulfate was found to be the major component of $PM_{2.5}$ and high magnitude AOIs to SO_2 emissions and lower ones to NO_x emissions. Ammonia was found to have a significant impact on Atlanta mainly from the formation of ammonium.

The AOI results are consistent with HYSPLIT model trajectories for sources of air parcels that eventually impacted the receptor (Atlanta) on each day.

Acknowledgments

The support for this project came from U.S. Environmental Protection Agency under Agreements RD82897602, RD83107601, RD83096001.

References

Boylan, J.W., Odman, M.T., Wilkinson, J.G., Russell, A.G., 2004. Integrated Assessment Modeling of Atmospheric Pollutants in the Southern Appalachian Mountains: Part II—PM2.5 and Visibility. Georgia Institute of Technology.

Byun, D., Schere, K.L., 2006. Review of the governing equations, computational algorithms, and other components of the models-3 community multiscale air quality (CMAQ) modeling system. Applied Mechanics Reviews 59, 51–77.

CEP, 2004. Sparse matrix operator kernel emissions (SMOKE) modeling system. Carolina Environmental Programs, University of North Carolina, Research Triangle Park, NC. ⟨http://cf.unc.edu/cep/empd/products/smoke⟩.

Cohan, D.S., Hakami, A., Hu, Y., Russell, A.G., 2005. Nonlinear response of ozone to emissions: source apportionment and sensitivity analysis. Environmental Science and Technology 39, 6739–6748.

Dockery, D.W., Pope, C.A., Xu, X., Spengler, J.D., Ware, J.H., Fay, M.E., Ferris, B.G., Speizer, F.E., 1993. An association between air pollution and mortality in six U.S. Cities. The New England Journal of Medicine 329, 1753–1759.

Draxler, R.R., Rolph, G.D., 2003. HYSPLIT (Hybrid single-particle lagrangian intergrated trajectory) model access via NOAA ARL READY Website ⟨http://www.arl.noaa.gov/ready/hysplit4.html⟩. NOAA Air Resources Laboratory, Silver Spring, MD.

Dunker, A.M., Yarwood, G., Ortmann, J.P., Wilson, G.M., 2002a. Comparison of source apportionment and source sensitivity of ozone in a three-dimensional air quality model. Environmental Science and Technology 36, 2953–2964.

Dunker, A.M., Yarwood, G., Ortmann, J.P., Wilson, G.M., 2002b. The decoupled direct method for sensitivity analysis in a three-dimensional air quality model—Implementation, accuracy, and efficiency. Environmental Science and Technology 36, 2965–2976.

Fine, J., Vuilleumier, L., Reynolds, S., Roth, P., Brown, N., 2003. Evaluating uncertainties in regional photochemical air quality modeling. Annual Review of Environment and Resources 28, 58–106.

Habermacher, F.D., Napelenok, S.L., Akhtar, F., Hu, Y., Russell, A.G., 2007. Area of influence (AOI) development:

fast generation of receptor-oriented sensitivity fields for use in regional air quality modeling. Environmental Science and Technology, in press.

Hakami, A., Seinfeld, J.H., Chai, T.F., Tang, Y.H., Carmichael, G.R., Sandu, A., 2006. Adjoint sensitivity analysis of ozone nonattainment over the continental United States. Environmental Science and Technology 40, 3855–3864.

Hu, Y., Cohan, D.S., Odman, M.T., Russell, A.G., 2004. Air quality modeling of the August 11–20, 2000 Episode for the Fall Line Air Quality Study. School of Civil and Environmental Engineering, Georgia Institute of Technology, Atlanta, GA.

Kim, S., Shen, S., Sioutas, C., Zhu, Y.F., Hinds, W.C., 2002. Size distribution and diurnal and seasonal trends of ultrafine particles in source and receptor sites of the Los Angeles basin. Journal of the Air and Waste Management Association 52, 297–307.

Napelenok, S.L., Cohan, D.S., Hu, Y., Russell, A.G., 2006. Decoupled direct 3D sensitivity analysis for particulate matter (DDM-3D/PM). Atmospheric Environment 40, 6112–6121.

NPS, 2006. National Park Service Air Quality Research Division, Fort Collins. Anonymous ftp at ⟨ftp://alta_vista.cira.colostate.edu in/data/improve⟩.

Pope, C.A., Burnett, R.T., Thun, M.J., Calle, E.E., Krewski, D., Ito, K., Thurston, G.D., 2002. Lung cancer, cardiopulmonary mortality, and long-term exposure to fine particulate air pollution. Journal of the American Medical Association 287, 1132–1141.

PSU/NCAR, 2003. PSU/NCAR mesoscale modeling system tutorial class notes and user's guide: MM5 modeling system version 3. Mesoscale and Microscale Meteorology Division, National Center for Atmospheric Research.

Russell, A.G., Dennis, R., 2000. NARSTO ciritical review of photochemical models and modeling. Atmospheric Environment 34, 2283–2324.

Sandu, A., Daescu, D.N., Carmichael, G.R., Chai, T.F., 2005. Adjoint sensitivity analysis of regional air quality models. Journal of Computational Physics 204, 222–252.

Seigneur, C., Pun, B., Chen, S.-Y., Lohman, K., 2004. Performance evaluation of four air quality models applied for an annual simulation of PM over the western United States. Atmospheric & Environmental Research, Inc., San Ramon, CA.

US-EPA, 1993. Aerometric information retrieval system (AIRS). Office of Air Quality Planning and Standards, Research Triangle Park, NC.

US-EPA, 1999. Draft Guidance on the Use of Models and Other Analysis in Attainment Demonstrations for the 8-Hour Ozone NAAQS.

US-EPA, 2004. Air quality criteria for particulate matter. EPA/600/P-99/002aF.

Yang, Y.J., Wilkinson, J.G., Russell, A.G., 1997. Fast, direct sensitivity analysis of multidimensional photochemical models. Environmental Science and Technology 31, 2859–2868.